

Weak ferromagnetism with very large canting in a chiral lattice: (pyrimidine)₂FeCl₂

R. Feyerherm, A. Loose

*Hahn-Meitner-Institut and Berlin Neutron Scattering Center, 14109 Berlin, Germany**

T. Ishida, T. Nogami

Department of Applied Physics and Chemistry, The University of Electro-Communications, Chofu, Tokyo 182-8585, Japan

J. Kreitlow, D. Baabe, F. J. Litterst, S. Süllow, H.-H. Klauss

*Institut für Metallphysik und Nukleare Festkörperphysik,
TU Braunschweig, 38106 Braunschweig, Germany*

K. Doll

Institut für Mathematische Physik, TU Braunschweig, 38106 Braunschweig, Germany

(Dated: November 1, 2018)

The transition metal coordination compound (pyrimidine)₂FeCl₂ crystallizes in a chiral lattice, space group $I4_122$ (or $I4_322$). Combined magnetization, Mössbauer spectroscopy and powder neutron diffraction studies reveal that it is a canted antiferromagnet below $T_N = 6.4$ K with an unusually large canting of the magnetic moments of 14° from their general antiferromagnetic alignment, one of the largest reported to date. This results in weak ferromagnetism with a ferromagnetic component of 1 μ_B . The large canting is due to the interplay between the antiferromagnetic exchange interaction and the local single-ion anisotropy in the chiral lattice. The magnetically ordered structure of (pyrimidine)₂FeCl₂, however, is not chiral. The implications of these findings for the search of molecule based materials exhibiting chiral magnetic ordering is discussed.

PACS numbers: 75.25.+z; 75.50.Ee; 75.50.Xx

I. INTRODUCTION

One major research effort in the very active field of molecule based magnetic materials^{1,2,3,4,5} is directed towards synthesizing multifunctional compounds that combine magnetism with a second physical property, such as conductivity⁶ or optical activity.⁷ In this framework, extensive efforts are undertaken to find chiral magnetic materials that exhibit magnetochemical dichroism (MChD), a phenomenon first observed by Rikken and Raupach in a chiral paramagnetic material.⁸ Large MChD is expected in materials that combine chirality and magnetic order. To date, however, there is no evidence for large MChD, although a number of chiral magnetic materials have been reported.⁹

Recently, the magnetism of pyrimidine bridged transition metal complexes has been investigated in which pyrimidine ($C_4H_4N_2$), in the following abbreviated as PM, plays the role of an antiferromagnetic coupling unit.^{10,11,12,13} Interestingly, the halide complexes (PM)₂TX₂ (T = Co^{II}, X = Cl, Br; T = Fe^{II}, X = Cl) possess a chiral 3-dimensional network of T ions and exhibit weak ferromagnetism below about 5 K.^{14,15} The preliminary analysis of magnetization measurements on these compounds pointed to a very large canting and an associated large ferromagnetic component of the ordered moments. It appeared possible that these compounds possess a chiral magnetically ordered structure.

In order to determine the magnetic structure and to elucidate the origin of the large canting we performed magnetization measurements, Mössbauer spectroscopy

and powder neutron diffraction on (PM)₂FeCl₂. Here, we present a complete analysis of these data together with electronic structure calculations. We discuss the implications of our findings for studies in search of molecule based materials exhibiting chiral magnetic ordering.

II. EXPERIMENTAL

Microcrystalline samples of (PM)₂FeCl₂, in the following abbreviated PFC, were obtained by mixing aqueous solutions of Fe^{II} chloride (e.g. 10 mmol in 20 ml H₂O) with the stoichiometric amount of pyrimidine. The resulting yellow precipitates were filtered and washed thoroughly with H₂O. Mössbauer data indicate the presence of a secondary phase, which we identified as (PM)FeCl₂. The volume amount of the secondary phase increases with storage time of the samples. While a newly made sample contained less than 2% secondary phase, about 22% secondary phase have been observed in the same sample stored for two years under air. This indicates that under such conditions PFC is unstable against the formation of (PM)FeCl₂. Magnetization measurements were carried out using an MPMS Squid magnetometer (Quantum Design). Some 20 mg of freshly prepared sample was filled into a gelatine capsule. ⁵⁷Fe Mössbauer spectroscopy experiments have been executed in a standard low-temperature Mössbauer set-up at temperatures ranging from 3 K to 300 K (source: ⁵⁷Co-in-Rh matrix at room temperature; half width half maximum (HWHM): 0.130(2) mm/s). The spectra have been evaluated us-

ing the Mössbauer fitting program Recoil¹⁶ in the thin absorber approximation. Above T_N the spectra were modeled as Lorentzian lines in the presence of an electric field gradient. Below T_N we employed a method for the calculation of Mössbauer line shapes in the presence of magnetic dipole and electric quadrupole hyperfine interactions introduced by Blaes *et al.*¹⁷ Neutron powder diffraction measurements were performed using the instruments E6 and E9 at the Berlin Neutron Scattering Center (BENSC). Neutron wavelengths of 2.448 Å and 1.7964 Å, respectively, were used. The instrument E6 provides a high neutron flux and medium resolution, is equipped with a 20°-multichannel detector, and covers a range of scattering angles up to about 100°. In contrast, the instrument E9 is a low-flux high-resolution powder diffractometer with an extended 2θ -range up to 160°. Therefore, the former was used for the study of magnetic Bragg reflections, while the latter was employed for checking the crystal structure at low temperatures. The non-deuterated sample was filled into a 7 mm diameter vanadium can with 40 mm length, resulting in a sample volume of about 1.5 cm³. An absorption correction for cylindrical samples was applied ($\mu R = 0.94$) to account for the strong incoherent scattering from hydrogen. During the refinement, no other but symmetry constraints were used for the atom positional parameters. Therefore, the validity of the crystal structure model is proven by the correct geometry of the pyrimidine molecules determined in the refinement. The Rietveld refinement of the diffraction data was carried out using the WIN-PLOTR/FULLPROF package.¹⁸

III. THEORETICAL CALCULATIONS

The electronic structure calculations were performed with a code based on a local basis set.¹⁹ The unrestricted Hartree-Fock method and the hybrid functional B3LYP is applied for solids, and the basis functions are chosen as Gaussian type orbitals. The iron basis set²⁰ (outermost d -exponent 0.4345) is of the size [5s4p2d], the chlorine basis set²¹ (with one d -exponent with value 0.5) of the size [5s4p1d], carbon and nitrogen basis sets²² of the size [3s2p1d], and finally a [2s1p] hydrogen basis set²³ was used. To test the stability of the results, additional tight basis functions were added for the iron atoms and a diffuse sp -function (exponent 0.12) was added at the nitrogen site to account for a better description of this negatively charged atom. The results were, however, found to be essentially stable with respect to the various basis sets. With these parameters, the Hartree-Fock or Kohn-Sham equations for a ferro- or antiferromagnetic (Neel-like) structure are solved self-consistently, and properties such as charge distributions and field gradients can be computed. The structural data used in the calculations is based on the measurements as described in the following.

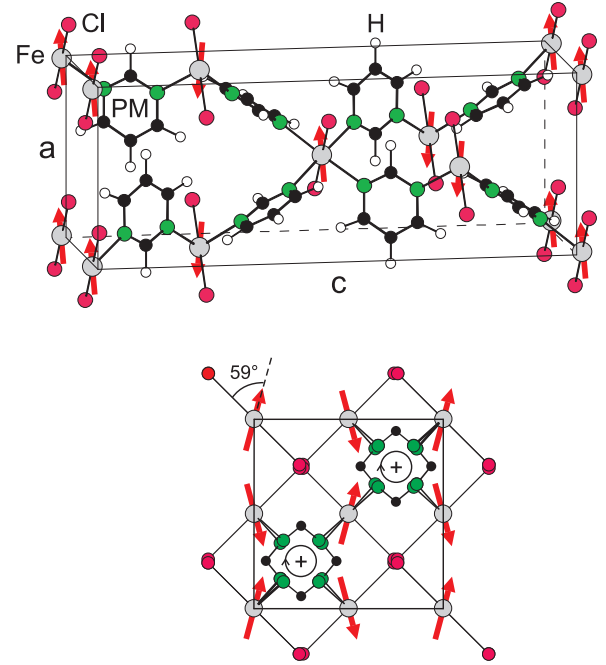


FIG. 1: Crystal and magnetic structure of PFC as determined from low-temperature powder neutron diffraction. Lower section: view along the c axis with the positions of the 90° screw axes marked. The angle 59° between the magnetic moments and the local EFG is also marked.

IV. RESULTS AND DISCUSSION

A. Crystal structure

The high-resolution powder neutron diffraction data, taken at 10 K, confirm that PFC is isostructural to the Co analogue¹⁴, namely tetragonal with the chiral space group $I4_122$ (or the enantiomeric $I4_322$) with $a = b = 7.4292(3)$ Å, $c = 20.364(1)$ Å. The Fe-N and Fe-Cl distances 2.26 and 2.39 Å are determined, respectively. The crystal structure is shown in Fig. 1. It consists of a chiral three-dimensional network of Fe ions coordinated by two Cl and linked by pyrimidine. Due to the 4₁ (or 4₃) screw axis, the local environment of two Fe ions in neighboring layers z and $z + 1/4$ is rotated by 90°. We will discuss below that this specific feature of the crystal structure of PFC can be regarded as the origin of the large canting observed in the magnetically ordered state.

In the local FeN_4Cl_2 geometry all nitrogen atoms of pyrimidine are equatorially coordinated. It was pointed out¹³ that the electron spins in magnetic $d_{x^2-y^2}$ orbitals are antiferromagnetically correlated through the pyrimidine molecular orbital(s), i.e., by a superexchange mechanism,^{24,25,26,27} when the nitrogen lone pair and $d_{x^2-y^2}$ orbitals have an appreciable orbital overlap on both sides.

V. RESULTS AND DISCUSSION

A. Magnetization

Figure 2 shows the M vs. H hysteresis curve of PFC measured at 2.0 K. For clarity, the virgin curve is not shown. On increasing the field from zero, we observe an initial steep increase of the magnetization in a low field region (a few 100 Oe) to a value much smaller than the full Fe^{II} moment, and subsequently a rounded crossover around 500 Oe to a linear field dependence up to 55 kOe (not shown). Such a behavior is typical of a weak ferromagnet, where the steep increase at low T reflects the spontaneous magnetization and the linear high-field behavior is due to strong antiferromagnetic interactions. On sweeping the field down from 55 kOe, a weak hysteresis develops and a sharp kink is observed at $H = 0$. This kink allows an accurate determination of the spontaneous magnetization. We determine a value of $0.31(1) \mu_B$ on the powder average. The coercitive field is small, 150 Oe, and therefore PFC behaves as a soft magnet. Assuming that the ferromagnetic component in a given magnetic domain is confined to a specific crystal direction, the measured powder average of the spontaneous magnetization has to be multiplied by a factor of three to obtain the ferromagnetic moment along this axis. This fact is frequently overlooked by other authors. Thus, the magnetization measurements result in a ferromagnetic component of $0.93(3) \mu_B$ per Fe ion in the canted antiferromagnetic state. We will show in the following that this value is in full agreement with the combined Mössbauer spectroscopy and neutron diffraction results.

B. Mössbauer spectroscopy

In Fig. 3 we plot the Mössbauer-spectra of PFC at temperatures between 3.75 K and 300 K. At highest temperatures we observe a two line spectrum, resulting from a quadrupole splitting of $QS = 3.12(3) \text{ mm/s}$ and an isomer shift of $IS = 0.909(1) \text{ mm/s}$ (relative to the ^{57}Co -in-Rh source). These values are typical for high spin Fe^{II} . Upon lowering the temperature, and above T_N , both QS and IS slightly increase, and we find at 10.4 K values of $QS = 3.271(2) \text{ mm/s}$ and $IS = 1.037(1) \text{ mm/s}$.

Below T_N , at 3.75 K, eight separate absorption lines are observed. These we attribute to the coexistence of an electrical field gradient (EFG) and a hyperfine magnetic field (B_{HF}). A fit to the data, taking into account the EFG, B_{HF} and the asymmetry parameter $\eta = (V_{xx} - V_{yy})/V_{zz}$ yields values of $IS = 1.035(3) \text{ mm/s}$, $\eta = 0.106$, $QS = 3.28(1) \text{ mm/s}$ and a hyperfine magnetic field of $30.19(3) \text{ T}$ as best solution. Moreover, from this fit we determine a temperature independent angle of B_{HF} with the main EFG component V_{zz} of $59.3(1)^\circ$ at each Fe site.

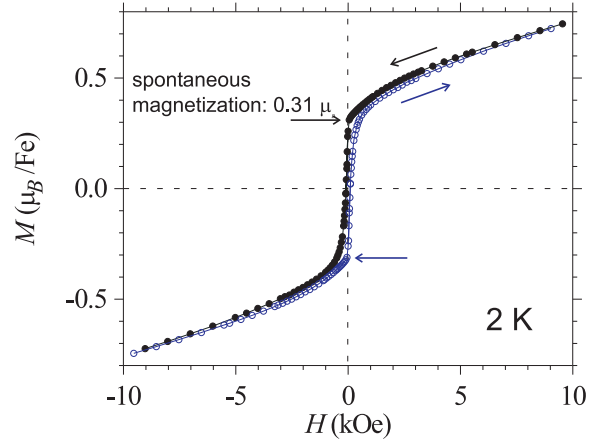


FIG. 2: Low-field section of the hysteresis-loop of PFC measured at 2 K. The field was swept between -55 kOe and 55 kOe. For clarity, the virgin curve is not shown. Horizontal arrows mark sharp kinks allowing for the determination of the spontaneous magnetization.

C. Results from calculations

From the calculations, the charges were determined to be +1.9 for Fe, -1.0 for Cl, -0.8 for N; between 0 and +0.7 for carbon, and the hydrogen atoms were found to be slightly positive charged (at most +0.1). The spin at the Fe sites is 1.9 and the magnetic moment $4.04 \mu_B$, using a g -factor of 2.13.¹⁵ Thus, there is moment reduction by about 5% due to covalency effects. The magnitude of the spin at the Cl, N or C sites is less than 0.1 and thus negligible, and the spin at the hydrogen sites virtually zero. The electric field gradient at the Fe site has components with the value $V_{xx} = -0.8$, $V_{yy} = -1.3$, and $V_{zz} = 2.1 \times 10^{22} \text{ V/m}^2$. These numbers have an uncertainty of the order of $0.1 \times 10^{22} \text{ V/m}^2$. The asymmetry parameter η is especially sensitive to this uncertainty and values in the range from 0.1 to 0.3 are obtained.

The second largest component of the tensor is identical with the crystallographic c -direction, the other two components lie perpendicular in the tetragonal basal plane and are rotated by 45° with respect to a and a' . The largest component is in the direction of the Cl atoms. We can compare the computed field gradient with the experimental value by converting according to the formula $QS = eQV_{zz}c/2E_0$, with $E_0 = 14.4 \text{ keV}$ and using the value of 0.16 barn for the quadrupole moment Q .²⁸ With these parameters, we obtain a computed $QS = 3.5 \text{ mm/s}$ which is in good agreement with the experimental value. Finally, it is worthwhile mentioning that the aforementioned calculated values hardly depend on the magnetic ground state, and similar values are obtained if a ferromagnetic or an antiferromagnetic ground state is assumed.

An attempt to extract information about the magnetic exchange coupling could be made by comparing energies

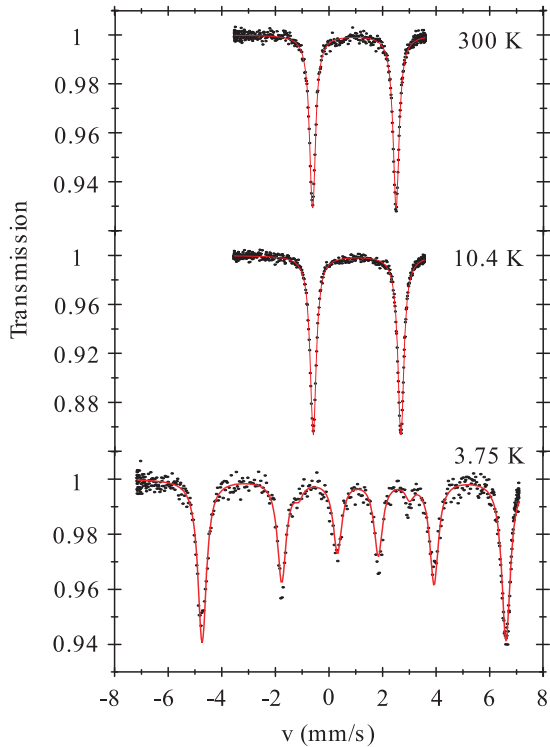


FIG. 3: Mössbauer spectra of PFC measured at various temperatures. Arrows mark eight absorption lines observed at 3.75 K. The solid lines are fits to the data points (see text).

for ferro- and antiferromagnetic structure. This difference is (per Fe ion) roughly 0.01 eV at the HF level (with the ferromagnet being lower), and roughly 0.08 eV at the B3LYP level (with the antiferromagnet being lower). However, these energies should be of the order of the Neel temperature (6.4 K or 0.6 meV). The large deviation could be due to the fact that a simplified magnetic order is used in the simulations, neglecting the canting, or that the description of the electronic correlations is too crude due to the approximations in the functional. If the HF result was assumed to be reasonable, then the effect of electronic correlations would have to be of virtually the same size, but with opposite sign. Such a subtle effect is very difficult to be computed properly, and a density functional calculation may be too crude.

D. Magnetic structure

Figure 4 shows the difference of the powder neutron diffractograms taken at 1.6 and 7 K (i.e., well below and above T_N), revealing the additional Bragg intensities produced by the long-range magnetic ordering. All magnetic reflections can be indexed on the basis of the crystallographic unit cell. The rule $h + k + l =$ even for the observed magnetic Bragg reflections (hkl) indicates that the body centering is conserved. The presence and

strengths of the reflections $(00l)$ suggest that the magnetic moments lie basically perpendicular to the c axis and that moments in neighboring layers z and $z+1/4$ are basically oriented antiparallel. Therefore, the antiferromagnetic coupling through pyrimidine bridges is clearly indicated.

First refinements of the neutron diffraction data resulted in an ordered moment of roughly $4 \mu_B$ at 1.6 K. However, the orientation of the moments within the basal plane as well as the angle and direction of canting can not be determined from these data since the only clear signature of the ferromagnetic component is the weak (112) reflection which is hidden in the noise. We therefore used the information from the Mössbauer spectroscopy to arrive at the final magnetic structure model.

Assuming the electric field gradient parallel to the Fe-Cl bonds, as it was determined in the calculations, in the basic antiferromagnetic structure the moments have to be aligned parallel to the a axis in order to enclose an identical angle with the local EFG at each Fe. To increase this angle from 45° to 59.3° - as observed in the Mössbauer experiment - either a canting by 14.3° within the basal plane (along a') or by 45° along c has to be introduced. However, only a canting in the basal plane gives a ferromagnetic component close to $1 \mu_B$, whereas a canting along c would require a ferromagnetic component of $2.8 \mu_B$. Comparing these values to the results from the magnetization measurements, the latter model can be clearly ruled out. Therefore, in the final magnetic structure model, the moments were confined to the basal plane and the canting angle 14.3° was fixed. The solid line in Figure 4 is a fit of this final model to the data. The only free parameter is the magnitude of the ordered moment. All other parameters, such as lattice constants and lineshapes, were taken from the fit of the nuclear Bragg pattern recorded at 7 K (not shown).

Given the large background noise from the hydrogen incoherent scattering, it gives a good agreement with the data ($R_p = 0.114$, $R_{wp} = 0.137$). The fit yields an ordered moment of $4.0(3) \mu_B$ - in agreement with the above calculated full moment on the Fe - and a ferromagnetic component of $1.0(1) \mu_B$. The latter value is in good agreement with the magnetization data.

The temperature dependence of the intensity of the (002) Bragg reflection is shown in Figure 5 together with the corresponding data, the square of the hyperfine field B_{HF} , from the Mössbauer experiment. It decreases continuously with rising temperature and vanishes at $6.4(2)$ K. Assuming that the canting angle is constant, the Bragg intensity is proportional to the square of the ordered moment. A fit of the region close to T_N with a power law is consistent with a critical exponent of $\beta = 0.36(1)$ and therefore with 3D Heisenberg behavior.

The canting angle $\alpha = 59.3^\circ - 45^\circ = 14.3^\circ$ observed in the present measurements is extremely large, actually one of the largest reported to date for any weak ferromagnetic compound. For example, weak ferromagnetism of Fe with a canting angle of 16° has been reported for

the intermetallic compound UFe_4Al_8 . However, the ferromagnetic component is only $0.3 \mu_B$ per Fe in this compound and the canting is due to an interaction between the U $5f$ and the Fe $3d$ electrons.²⁹ Therefore, the physics of this compound is hardly comparable to that of PFC.

Large canting angles of $2\text{--}7^\circ$ have been also observed in Gd_2CuO_4 -type cuprates. For these materials, a correlation between weak ferromagnetism and the crystal symmetry has been discussed in detail.³⁰ We believe that such a correlation is also present in PFC and that the large canting observed in this compound is a direct result of its chiral lattice symmetry. Due to this symmetry, the orientation of the local easy axis varies by 90° between nearest Fe neighbors linked by a pyrimidine molecule. Therefore, the local anisotropy would favor a 90° alignment between the moments. However, the AFM interaction favors a 180° alignment. The actual angle $180^\circ - 2\alpha = 151.4^\circ$ between neighboring moments therefore can be regarded as the result of the competition of the local anisotropy and the antiferromagnetic exchange. The final magnetic structure model suggests that the local easy axis lies perpendicular to c and within the equatorial plane of the local coordination octahedron of each Fe. Thus, it coincides with the axis of the smallest EFG component V_{xx} calculated above. We may express this anisotropy as an additional term in the Hamiltonian of the system,

$$\mathbf{H} = \sum_{NN} [J\vec{S}_1 \cdot \vec{S}_2 + D(S_{1x}S_{2y})], \quad (1)$$

where the sum is over all pairs of nearest neighbor (NN) spins (\vec{S}_1, \vec{S}_2), $\vec{S}_j = (S_{jx}, S_{jy}, S_{jz})$, and $D < 0$. The resulting angle α is related to D and J by $D/J = -2 \sin 2\alpha$. With the measured α we get $D = -0.96J$. If one would assign the canting to a Dzyaloshinsky-Moriya (DM) type interaction,^{31,32,33} the DM vector was aligned along c as expected for symmetry reasons and the DM term would read $D(S_{1x}S_{2y} - S_{1y}S_{2x})$. The latter term of (1) differs from the DM term in leading to a canting towards specific axes x and y for S_1 and S_2 , respectively, rather than a canting within the tetragonal basal plane in general.

It is interesting to note that magnetization data on the Co analogues to PFC, $(\text{PM})_2\text{CoCl}_2$ and $(\text{PM})_2\text{CoBr}_2$,¹⁴ point to even larger ferromagnetic components and therefore even larger canting angles than in PFC. Another example of such a large canting may be 3D-[Fe(N_3)₂(4,4'-bpy)], with bpy = 4,4'-bipyridine. A microcrystalline sample of this compound was recently reported to exhibit a large spontaneous magnetization of $0.48 \mu_B$ per Fe tentatively ascribed to ferromagnetic ordering while a canted structure was not excluded.^{34,35} This tetragonal compound also forms a chiral 3D network structure, space group $P4_12_12$, which is closely related to that of $(\text{PM})_2\text{FeCl}_2$. The negative Curie-Weiss temperature and the similarity of the magnetization data of 3D-[Fe(N_3)₂(4,4'-bpy)] with that of the $(\text{PM})_2\text{TX}_2$ complexes suggests that also in the former a canted antifer-

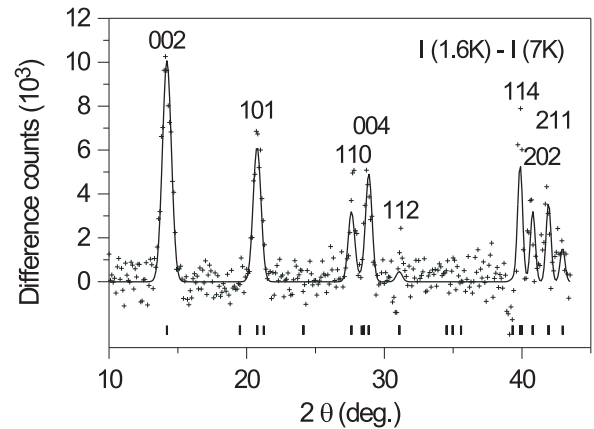


FIG. 4: Difference of the two neutron powder diffractograms measured at 1.6 K (below T_N) and 7.0 K (above T_N) for PFC. The wavelength was 2.448 Å. The reflections are indexed on the basis of the crystallographic unit cell.

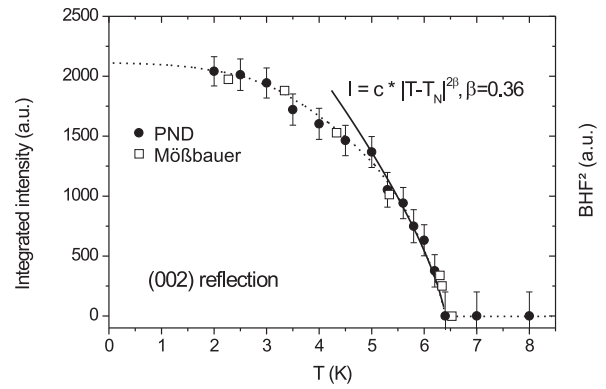


FIG. 5: Temperature dependence of integrated intensity of the (002) Bragg reflection, being proportional to the square of the ordered moment, together with the hyperfine field B_{HF} observed by Mössbauer spectroscopy. The dashed line is a guide to the eye. The solid line is a fit to a power law which is consistent with 3D Heisenberg behavior.

romagnetic state with a very large canting (of roughly 20°) within the tetragonal basal plane is realized.

To our knowledge, only few other molecule based magnets with chiral crystal structures have been reported. The oxalato (ox) based compound $[\text{Co}(2,2'\text{-bpy})_3][\text{Co}_2(\text{ox})_3]\text{ClO}_4$ ³⁶ exhibits weak ferromagnetism with small canting ($\mu_{\text{fm}} = 0.009 \mu_B$). The compounds of the series $[\text{Z}^{\text{II}}(2,2'\text{-bpy})_3][\text{ClO}_4][\text{M}^{\text{II}}\text{Cr}^{\text{III}}(\text{ox})_3]$ ³⁷ order ferromagnetically. Both systems crystallize in the cubic chiral space group $P4_132$. Another example is ferrimagnetic $\text{Mn}(\text{hfac})_2\text{NITPhOMe}$, crystallizing in space group $P3_1$.³⁸ The other compounds discussed in the framework of chiral magnetism are based on chiral constituents and crystallize in non-centrosymmetric but achiral space groups, such as $P1$ or $P2_12_12_1$.⁹

VI. CONCLUSION

We have shown that $(\text{PM})_2\text{FeCl}_2$ is a weak ferromagnet with low coercitive field but a very large ferromagnetic component of $1 \mu_B$, corresponding to a canting angle of 14° . This is one of the largest values reported to date. In a given magnetic domain, the antiferromagnetic component of the moments is confined to the a axis, while the canting occurs along the perpendicular direction a' . We argued that the large canting in PFC is the direct result of its chiral lattice symmetry leading to a competition between the antiferromagnetic exchange interaction and the local single-ion anisotropy. The appearance of canting rather than a chiral magnetic structure may be a general feature of the magnetic ordering in similar structures possessing 90° screw axes. This observation is of interest in view of the extensive efforts to produce a molecular magnet exhibiting chiral magnetic ordering. To date, both strategies, crystallizing (i) achiral constituents in a chiral lattice and (ii) chiral constituents

in non-centrosymmetric but achiral lattices did not lead to chiral magnetic ordering.

Most of these compounds possess 90° or 180° screw axes. These lead to a $\pm 90^\circ$ or to no alteration at all, respectively, of the local anisotropy along the screw axes and thus do not necessarily support any chirality of the ordered magnetic structure. Local anisotropy supporting chiral magnetic ordering therefore appears more likely in chiral trigonal/hexagonal lattices. We suggest that the search for chiral magnetic ordering should focus on compounds of that kind.

Acknowledgments

We thank N. Stuesser and D. Toebbens for experimental support. This work has been supported by the Deutsche Forschungsgemeinschaft DFG under contract no. SU229/6-1.

* Electronic address: Feyerherm@hmi.de

¹ *Proc. of ICMM 2000* (2001), in *Polyhedron* **20**, pp. 1115–1784.

² *Proc. of ICMM 2002* (2003), in *Polyhedron*, in press.

³ O. Kahn, *Molecular Magnetism* (VCH, New York, 1993).

⁴ J. Miller and A. Epstein, *Angew. Chemie* **106**, 399 (1994).

⁵ D. Gatteschi, *Adv. Materials* **6**, 635 (1994).

⁶ E. Coronado, J. P. Galán-Mascarós, C. J. Gómez-García, and V. Laukhin, *Nature* **408**, 447 (2000).

⁷ S. Benard, P. Yu, J. Rivière, R. Clément, J. Guilhelm, L. Tchernatov, and K. Nakatani, *J. Am. Chem. Soc.* **122**, 9444 (2000).

⁸ G. L. J. A. Rikken and E. Raupach, *Nature* **390**, 493 (1997).

⁹ E. Coronado, C. J. Gómez-García, A. Nuez, F. M. Romero, E. Rusanov, and H. Stoeckli-Evans, *Inorg. Chem.* **41**, 4615 (2002), and references therein.

¹⁰ T. Ishida, S.-I. Mitsubori, T. Nogami, and H. Iwamura, *Mol. Cryst. Liq. Cryst.* **233**, 345 (1993).

¹¹ G. D. Munno, T. Poerio, M. Julve, F. Lloret, and G. Viau, *New J. Chem.* p. 299 (1998).

¹² R. Feyerherm, S. Abens, D. Günther, T. Ishida, M. Meißner, M. Meschke, and T. Nogami, *J. Phys.: Condens. Matter* **39**, 8495 (2000).

¹³ F. Mohri, K. Yoshizawa, T. Yamabe, T. Ishida, and T. Nogami, *Mol. Engineer.* **8**, 357 (1999).

¹⁴ K. Nakayama, T. Ishida, R. Takayama, D. Hashizume, M. Yasui, F. Iwasaki, and T. Nogami, *Chem. Lett.* p. 497 (1998).

¹⁵ K. Zusai, T. Kusaka, T. Ishida, R. Feyerherm, M. Steiner, and T. Nogami, *Mol. Cryst. Liq. Cryst.* **343**, 127 (2000).

¹⁶ K. Lagarec, Department of Physics University of Ottawa **Version 1.02** (1998).

¹⁷ N. Blaes, H. Fischer, and U. Gonser, *Nucl. Instr. and Meth. in Phys. Res. B* **9**, 201 (1985).

¹⁸ T. Roisnel and J. Rodríguez-Carvajal, *Materials Science Forum* **378-381**, 118 (2001).

¹⁹ V. R. Saunders, R. Dovesi, C. Roetti, M. Causá, N. M. Harrison, R. Orlando, and C. M. Zicovich-Wilson, *CRYSTAL98 User's Manual*, Theoretical Chemistry Group, University of Torino (1998).

²⁰ M. Catti, G. Valerio, and R. Dovesi, *Phys. Rev. B* **51**, 7441 (1995).

²¹ M. Prencipe, A. Zupan, R. Dovesi, E. Aprá, and V. R. Saunders, *Phys. Rev. B* **51**, 3391 (1995).

²² R. Dovesi, M. Causá, R. Orlando, C. Roetti, and V. R. Saunders, *J. Chem. Phys.* **92**, 7402 (1990).

²³ R. Ditchfield, W. J. Hehre, and J. A. Pople, *J. Chem. Phys.* **54**, 724 (1971).

²⁴ J. Kanamori, *J. Phys. Chem. Solids* **10**, 87 (1959).

²⁵ A. P. Ginsberg, *Inorg. Chim. Acta Rev.* **5**, 45 (1971).

²⁶ J. B. Goodenough, *Phys. Rev.* **100**, 564 (1955).

²⁷ J. B. Goodenough, *J. Phys. Chem. Solids* **6**, 287 (1958).

²⁸ P. Dufek, P. Blaha, and K. Schwarz, *Phys. Rev. Lett.* **75**, 3545 (1995).

²⁹ J. A. Paixão, B. Lebech, A. P. Gonçalves, P. J. Brown, G. H. Lander, P. Burlet, A. Delapalme, and J. C. Spirlet, *Phys. Rev. B* **55**, 14370 (1997).

³⁰ H. M. Luo, Y. Y. Hsu, B. N. Lin, P. Chi, T. J. Lee, and H. C. Ku, *Phys. Rev. B* **60**, 13119 (1999).

³¹ I. Dzyaloshinsky, *J. Phys. Chem. Solids* **4**, 241 (1958).

³² T. Moriya, *Phys. Rev.* **117**, 635 (1960).

³³ T. Moriya, *Phys. Rev.* **120**, 91 (1960).

³⁴ T. Yuen, C. L. Lin, A. Fu, and J. Li, *J. Appl. Phys.* **91**, 7385 (2002).

³⁵ A. Fu, X. Huang, J. Li, T. Yuen, and C. L. Lin, *Chem. Eur. J.* **8**, 2239 (2002).

³⁶ M. Hernández-Molina, F. Lloret, C. Ruiz-Pérez, and M. Julve, *Inorg. Chem.* **37**, 4131 (1998).

³⁷ E. Coronado, J. P. Galán-Mascarós, C. J. Gómez-García, and J. M. Martínez-Agudo, *Inorg. Chem.* **40**, 113 (2001).

³⁸ A. Caneschi, D. Gatteschi, P. Rey, and R. Sessoli, *Inorg. Chem.* **30**, 3936 (1991).